

EUROPEAN ORGANIZATION FOR NUCLEAR RESEARCH

Proposal to the ISOLDE and Neutron Time-of-Flight Committee

Measurement of the inelastic scattering cross section of neutrons on ^{19}F by γ -ray spectroscopy

October 3, 2024

G. Lorusso¹, T. Wright², M. Birch^{1,2}, N. Colonna³, S. Amaducci⁴, M. Bacak^{2,5}, M. Boromiza⁴, L. Cosentino³, P. Finocchiaro³, D. Jenkins⁶, N. Kalantar-Nayestanaki⁷, M. Kavatsyuk⁷, A. Negret⁴, N. Patronis⁸, C. Petrone⁴, J. Praena⁸.

¹*National Physical Laboratory – Teddington, Middlesex, UK*

²*School of Physics and Astronomy, The University of Manchester, Manchester M13 9PL, UK*

³*INFN, sezione di Bari, Bari, Italy*

⁴*INFN Laboratori Nazionali del Sud, Catania, Italy*

⁴*Horia Hulubei National Institute for R&D in Physics and Nuclear Engineering, Romania*

⁵*European Organization for Nuclear Research (CERN), Switzerland*

⁸*University of Ioannina, Greece*

⁶*University of York, York, UK*

⁷*ESRIG, University of Groningen, Groningen, Netherlands*

⁸*University of Granada, Spain*

Spokesperson: G. Lorusso (giuseppe.lorusso@npl.co.uk), T. Wright (tobias.wright@manchester.ac.uk)

Technical coordinator: O. Aberle (oliver.aberle@cern.ch)

Abstract: Fluorine is a critical component of the molten salt Li_2BeF_4 (FLiBe), which has been widely proposed as a moderator and coolant material in nuclear applications. In fusion applications, FLiBe is attractive for its superior tritium breeding performance and low electrical conductivity. Advanced (GEN-IV) fission systems such as Fluoride-salt-cooled high-temperature reactors (FHRs) use FLiBe as coolant and molten salt reactors (MSRs) use FLiBe both as a solvent for fissile material and coolant.

This proposal aims to measure the $^{19}\text{F}(n,n')$ reaction cross section, whose current uncertainty due to scarce experimental data and discrepant model calculations has been found to propagate significantly on key aspects of fusion reactors modeling such as tritium breeding ratio and neutron flux. In FHR and MSR reactors it impacts reactivity calculations.

We propose to conduct the measurement at the EAR1 experimental area using an array



of LaBr₃ detectors which was recently commissioned at n_TOF. Using these detectors we will detect γ -rays following the de-excitation of ¹⁹F* states excited by the inelastic scattering of neutrons. The use of the n_TOF beam will allow to drastically reduce the existing uncertainty by collecting high neutron energy resolution data and in a much wider energy range than previously measured. This would provide a full set of experimental information to cover fission reactor applications and resolve main discrepancies between nuclear data libraries needed for fusion application.

Requested protons: 2×10^{18} protons on target
Experimental Area: EAR1

1 Scientific motivation

Tritium breeding blankets are a crucial component of fusion reactor designs, converting neutron energy into heat, shielding the magnets against radiation, cooling the first wall that separates the plasma from the blanket, and most importantly, to produce the ^3H fuel required to sustain reactor operation. The only element capable of producing enough ^3H via interaction with neutrons is Li (in particular ^6Li), but its reactivity with water, air and even reactor structural materials poses critical safety issues. The low melting point (180.5 °C) would force its use in a liquid form, bringing the additional problems of pressure losses due to magnetohydrodynamic (MHD) phenomena in the liquid metal while flowing in the high magnetic fields of the tokamak. For these reasons, Li compounds must be used instead, resulting in a decrease of Li atomic density that imposes additional constraints on breeding materials, such as low neutron parasitic absorption and capability of neutron multiplication.

Examples of promising Li compounds that have been selected based on the criteria of safety, low activation, availability, ^3H breeding and extraction efficiency are: (liquid) $\text{Li}_{17}\text{Pb}_{83}$ and LiBi_5Pb_4 , the salts Li_2BeF_4 (FLiBe) and LiF-NaF-BeF_2 (FLiNaBe), the (solid) intermetallic alloy Li_7Pb_2 , the Li ceramics Li_2O , LiAlO_2 , Li_2SiO_3 , Li_4SiO_4 , Li_2ZrO_3 , Li_2TiO_3 and non-ceramic binary compounds such as Li_3N and LiF .

This proposal, by measuring the neutron inelastic-scattering cross section of ^{19}F , addresses a specific nuclear data need for the molten-salt class of breeder material such as FLiBe. This is the best liquid salt for breeding tritium; beryllium multiplies neutrons via the $^9\text{Be}(n, 2n)$ reactions, and T production can be maximised using isotopically enriched ^6Li . The isotope ^7Li is also of interest, for example for its capability to produce T via the $(n, n'\alpha)^3\text{H}$ reaction without consuming neutrons. Therefore, a mixture of $^6\text{Li}/^7\text{Li}$ in FLiBe salts can be envisaged.

The FLiBe is also the best salt coolant in terms of thermal hydraulics and neutronic performance. For these reasons, FLiBe is the coolant of choice for liquid blankets in reactor designs with very high-magnetic-field where due to the much higher power density, it is difficult to cool solid blankets. In addition, the large magnetic field favours coolant in the blanket that have low electrical conductivity relative to Li-Pb to reduce interaction between flowing coolant and magnetic field.

Fluorine is also a critical element for a class of GEN-IV nuclear reactors known as molten salt reactor (MSRs). In this case the fuel is in solution of a molten salt (e.g., $\text{LiF-BeF}_2\text{-UF}_4$) which also serves as coolant, flowing through holes of a graphite moderator. A more recent concept is Fluoride salt-cooled High-temperature Reactors (FHRs), which feature high temperature fuel and fluoride salt coolant. The system uses pebble bed fuel and Li_2BeF_4 coolant enriched in ^7Li to minimize ^3H production. This concept is similar to high temperature gas reactors (HTGRs) but operates at near atmospheric pressure and with a power density 4-10 times higher.

Inelastic neutron scattering in fusion reactor components create high energy γ -rays that contributes to heat deposited and radiation damage. Furthermore, in both fusion/fission systems it affects the neutron energy spectrum, whose shape is critical to ^3H breeding. Sensitivity studies detailed in the following, show that the $^{19}\text{F}(n, n')$ uncertainty

propagates significantly in fusion/fission designs that use fluorine salt fuel/coolant. Fig. 1 shows a comparison between the only three existing measurements of the $^{19}\text{F}(n,n')$ reaction that observed the total inelastic cross section, along with available nuclear data libraries that in general show three trends. In the range 0.2-2.5 MeV there are two measurements performed with acceptable energy resolution and uncertainties of $\sim 15\%$ [1, 2, 3]. Three other measurements exist at higher energies but were not sensitive to the total cross section.

Fig. 1 shows a good agreement between Ref. [1] and the JENDL-5.0 library and there is in general a reasonable agreement between the three measurements. However, in the energy range 0.5-0.8 MeV, Ref. [2] reports a lower cross section that supports the JEFF-3.3/ENDF/B-VIII/TENDL2023 libraries. As a consequence, there is not enough evidence to recommend one of the two set of libraries. This situation causes a significant uncertainty in reactor calculations as described in the following. The Fusion Evaluated Nuclear Data Library (FENDL), specially aimed at fusion studies despite being the least supported by experimental data resembles more the JEFF-3.3 trend.

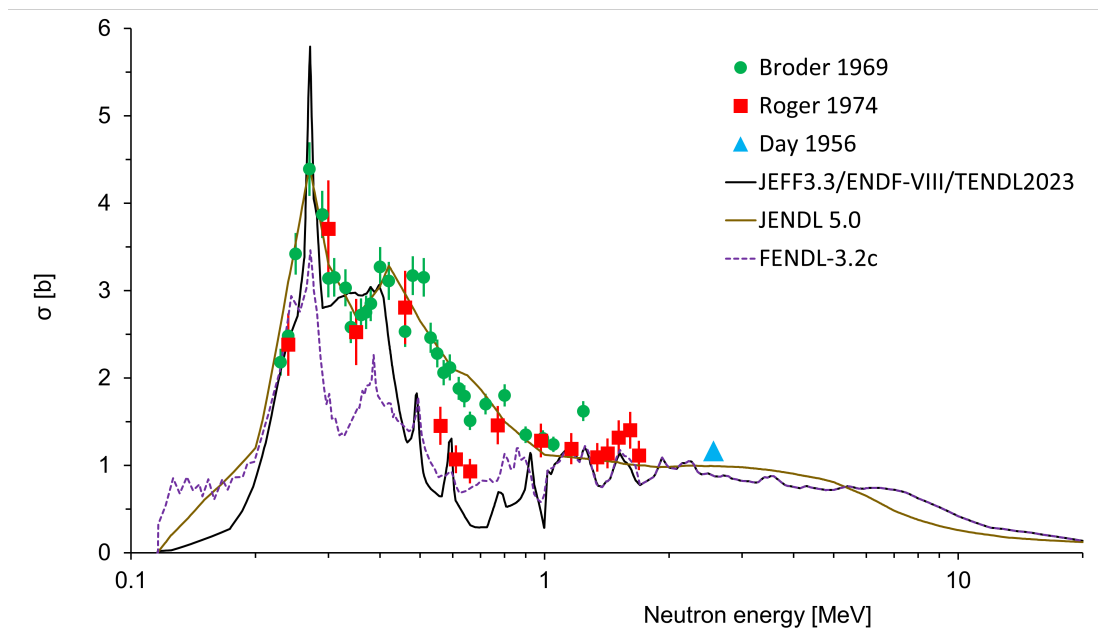


Figure 1: Three existing measurements of the total cross section of $^{19}\text{F}(n,n')$ compared to five nuclear data libraries.

A sensitivity study on the impact of this cross section for fusion application was conducted by the University of Wisconsin-Medison group, focused on the impact of the new FENDL-3.2c library in the case of a FLiBe liquid blanket reactor design [4]. The use of this library results in a 20-70% higher neutron flux behind the FLiBe breeder region (see Fig. 2). Also, the tritium breeding ratio increased by 1.4%. Considering the very low tolerances allowed in fusion design, this is considered a significant difference.

Ref. [5] reports a sensitivity studies on $^{19}\text{F}(n,n')$ for molten salt reactors focussed on

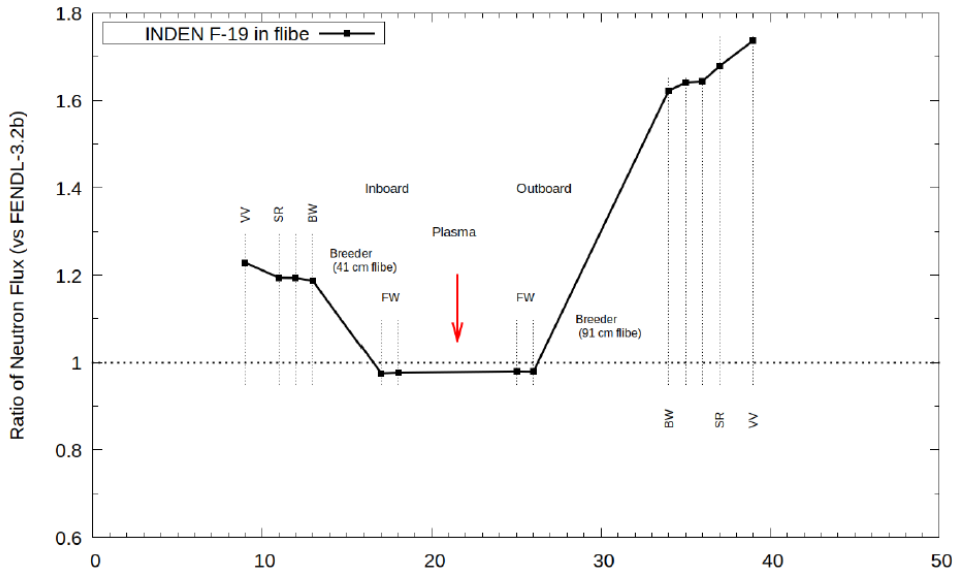


Figure 2: Ratio of neutron flux calculated using the FENDL and INDEN library. The vertical lines indicate the border between several parts of the fusion reactor surrounding the plasma (VV=vacuum vessel, SR=structural ring, BW=back wall, FW=first wall).

criticality uncertainty propagating from nuclear data. The system studied was a Thorium-TRU (TRans Uranium) fuel, explicitly, LiF-ThF₄-TRU-F₃ salt. The study focused on the difference between JENDL-4.0, JEFF-3.3 and ENDF/B-VIII.0. The results of the investigation illustrated in Fig. 3, were surprising, with the uncertainty of the ¹⁹F(n,n') cross section being the dominant one, and accounts for up to 2000 pcm.

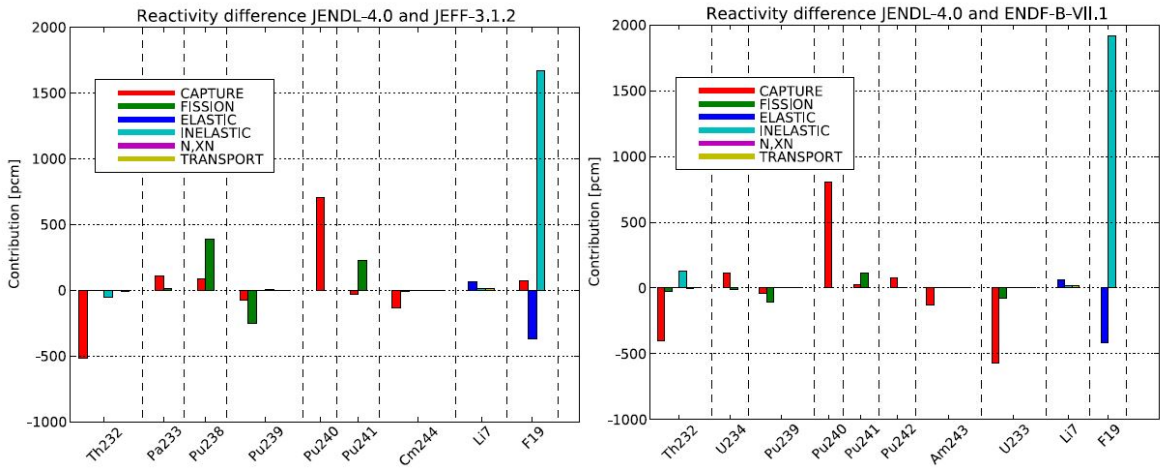


Figure 3: Reactivity difference due to different libraries to several key reactions for (left) JENDL/JEFF and JENDL/ENDF, showing the uncertainty in the inelastic scattering of ¹⁹F being a large effect.

A second study focused on a Fluorine based molten salt reactor, reported the contribution

MT	Label	Thermal		Epithermal	
		$\sigma_{\rho,MT}$ [pcm]	$\frac{\sigma_{\rho,MT}^2}{\sigma_{\rho,ALL}^2}$ [%]	$\sigma_{\rho,MT}$ [pcm]	$\frac{\sigma_{\rho,MT}^2}{\sigma_{\rho,ALL}^2}$ [%]
ALL	-	61.5	100.0	213.4	100.0
2	(n,elastic)	28.6	21.6	155.8	53.3
4	(n,inelastic)	9.3	2.3	113.9	28.5
16	(n,2n)	5.5	0.8	16.7	0.6
22	(n,na)	10.1	2.7	18.6	0.8
28	(n,np)	9.9	2.6	15.1	0.5
102	(n, γ)	34.1	30.7	53.4	6.2
103	(n,p)	11.0	3.2	19.9	0.9
104	(n,d)	5.7	0.9	15.5	0.5
105	(n,t)	10.1	2.7	16.7	0.6
107	(n, α)	42.7	48.2	138.5	42.1

Table 1: Reactivity uncertainty contributions in terms of absolute uncertainties and relative variances for the thermal and epithermal systems, when different reaction channels are perturbed individually.

of various ^{19}F reaction channels [6, 7]. The contribution of the uncertainty of the (n,n') channel was found to depend on the type of reactor regime: thermal, semi-epithermal, and epithermal. In the case of epithermal the contribution is greater because ^{19}F plays a larger role in slowing down neutrons. The results of the study is summarised in Table 1 below where the (n,n') channel contribution was 30% of the total and up to 114 pcm. To summarise, there is clear motivation to perform a new measurement of the $^{19}\text{F}(n, n')$ cross section. Sensitivity studies have been performed showing the large impact an improvement of the data would have for nuclear fission systems and the lack of data and prominence of ^{19}F in many fusion designs motivate an improvement of the data up to neutron energies relevant for both technologies (≤ 14.1 MeV).

1.1 Experimental setup and targets

The experimental setup consists of five LaBr_3 detectors 1.5" x 2" in size, mounted 15 cm away and at 125° degrees with respect to the beam as shown in Figure 4. This experimental setup was recently used to measure the $^{24}\text{Mg}(n, n')$ cross section and the detectors were able to resolve γ -rays originating from up to 100 MeV incident neutron energy. A LiF target of 2.5 g will be measured, providing a good compromise between sample mass and self-shielding. This has the advantage that it may also be possible to measure the cross section for the production of the 478 keV γ -ray in ^7Li which is an important measurement in itself.

1.2 Measurement details

Inelastic cross sections are typically measured by detecting γ -rays with HPGe detectors. However, the presence of a strong γ -flash, together with the intrinsically slow response

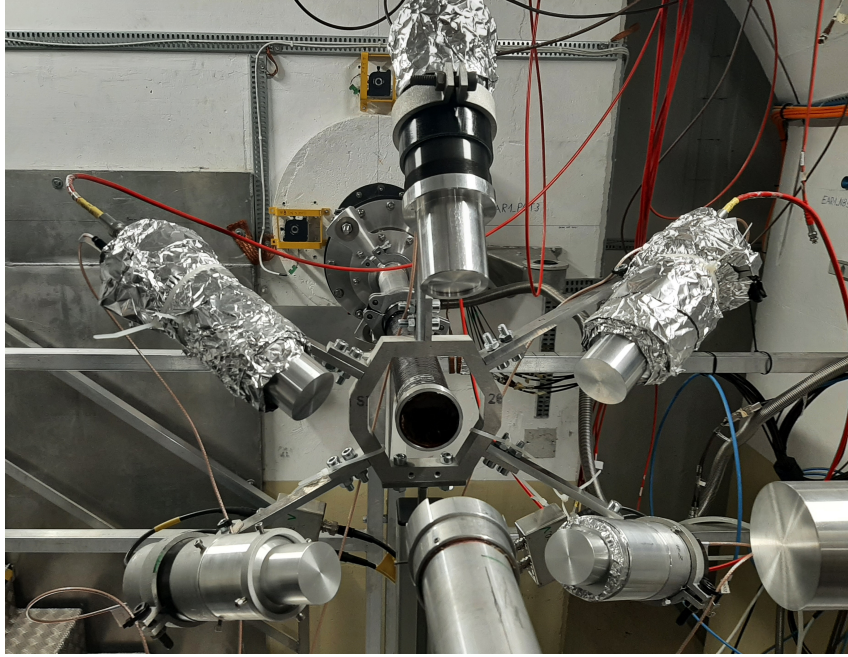


Figure 4: A photo of the experimental setup that will be used, shown here in use for the ^{24}Mg experimental campaign.

of such detectors, has hindered up to now the possibility to measure such reactions at n_TOF above 4-5 MeV neutron energy. To overcome this problem, the n_TOF Collaboration has recently proposed to use the much faster LaBr_3 detectors to extend the accessible neutron energy range in specific cases (mostly light isotopes), for which the line separation is larger than the 2-3% resolution of the detector. In these cases, tests performed with the neutron beam in EAR1@n_TOF have demonstrated the capability of a setup based on LaBr_3 detectors to measure inelastic reactions up to at least 100 MeV neutron energy. It should be noted, however, that for low-energy γ -rays, the neutron sensitivity of the detector may represent a limitation.

A difficulty of neutron inelastic measurements in the MeV region is the (n,p) channel polluting contribution which can generate a β^- unstable residual which can then decay back to the target nucleus populating the same excited states as the inelastic reaction. The $^{19}\text{F}(n,p)^{19}\text{O}$ reaction produces a residual which is long-lived enough (26 s) so that its β decay back to ^{19}F and subsequent excited states will be negligible. Also, even though ^{19}O is populated in several excited states which can decay through two intense lines with energies of 96 and 1375 keV, close to those of interest from ^{19}F , the (n,p) channel on ^{19}F is relatively weak compared to inelastic. Another relatively intense channel is (n, α) which forms ^{16}N (β^- unstable, decays mostly to second excited state in ^{16}O which decays through a 6128 keV line). This reaction mostly populates lower-lying states in ^{16}N that decay through the emission of 120, 298 and 276 keV γ -rays. These, however, should be fairly well separated from those of ^{19}F (109 and 197 keV). Similar arguments can be put forward also for the $^{19}\text{F}(n,d)^{18}\text{O}$.

The $^{19}\text{F}(n,2n)^{18}\text{F}$ channel has a reasonable cross section above 10 MeV and ^{18}F has

intense lines around 1 MeV where the LaBr₃ have good efficiency. It therefore possible also to measure the $(n, 2n)$ channel on this target nucleus taking advantage of the high neutron flux above 10 MeV specific to n_TOF. Since the $(n, 2n)$ channel impacts the neutron multiplicity, this cross section is also relevant in fusion and fission applications. Moreover, data reported by previous measurements display a rather divergent behaviour and thus a new data set for this reaction channel may help in improving its evaluation.

The primary motivation of this measurement remains to measure the (n, n') cross section and thus MCNP6 simulations were carried out in order to understand the limits of the LaBr₃ setup at n_TOF. Fig. 5 shows that the contribution of ¹⁹F γ -rays is well above any background contributions. This visible contamination to the ¹⁹F spectrum primarily comes from neutron inelastic excitation of ^{79,81}Br, therefore is intrinsic to the use of these detectors and depends on the neutron scattering cross section of the sample.

Although LaBr₃ exhibit reasonable γ -ray resolution, it is still limited and often makes it difficult to measure cross sections up to high energies due to the increased number of excited states involved, and thus emitted γ -rays. Figures 5 and 6 show this limitation, i.e., γ -rays from ¹⁹F* states above 4 MeV (higher than the 7th) are not resolved. However, γ -rays stemming from the first 6 excited states can be detected up to neutron energies of at least 20 MeV. As we will show later, these states dominate the cross section in the energy of interest (up to \sim 14 MeV), hence the proposed measurement will be an important step forward for nuclear applications.

Furthermore, despite the limitation above, the LaBr₃ spectrum is still sensitive to the neutron energy, and considering that all branching ratios of ¹⁹F are very well known for each state, it may be possible to use a simulated response to measure cross sections for higher excitation energies by combining simulated and experimental spectra. This technique, however, would have to be developed, but we are not aware of any isotope that can be used as a reference for this case. This proposed measurement is a good case to investigate the potential of this novel technique. In a recent test using ²⁴Mg data collected in the detector commissioning runs, a good agreement between cross sections measured at n_TOF and data collected at GELINA up to 14 MeV neutron energy, demonstrated the capability of the proposed setup. Further development may be required on in the analysis of data at higher energy, where there are no reference data.

1.3 Beam time request

The aim of this measurement is to accurately measure the (n, n') cross section in the keV - 1 MeV region where discrepant data sets exist, and also to extend the neutron energy range up to several tens of MeV, in a region where the cross section is expected to drop significantly. In order to do this, the partial cross sections to populate as many energy levels as possible at higher neutron energies must be measured. The evaluated nuclear data library ENDF/B-VIII.0 [8] provides partial cross sections for the population of each excited state and these are shown in Figure 7. It is noted that although the situation is complex with many excited levels, the cross section is dominated initially by the population of the first two excited states and thus emission of their corresponding γ -rays (109.9 and 197.1 keV) and at higher energies is dominated by the same second

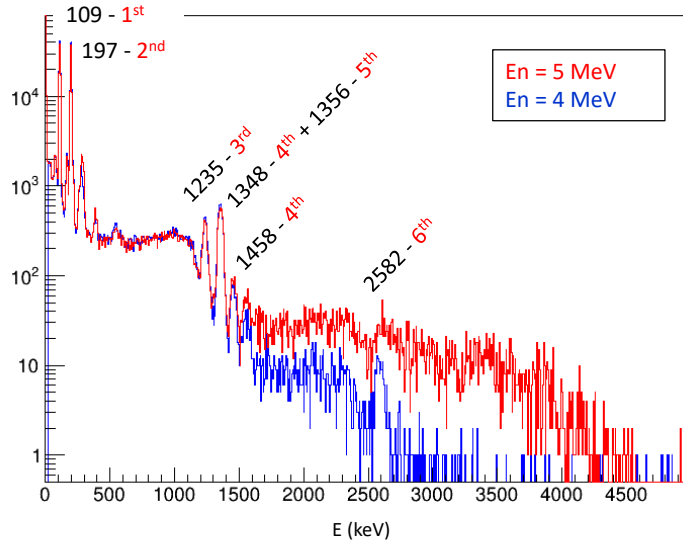


Figure 5: Simulated response of LaBr3 detector to 4 and 5 MeV neutrons. The γ -rays labeled with ordinal numbers are from the respective excited state in $^{19}\text{F}^*$. Any others originate from inelastic scattering in ^{139}La and $^{79,81}\text{Br}$ isotopes.

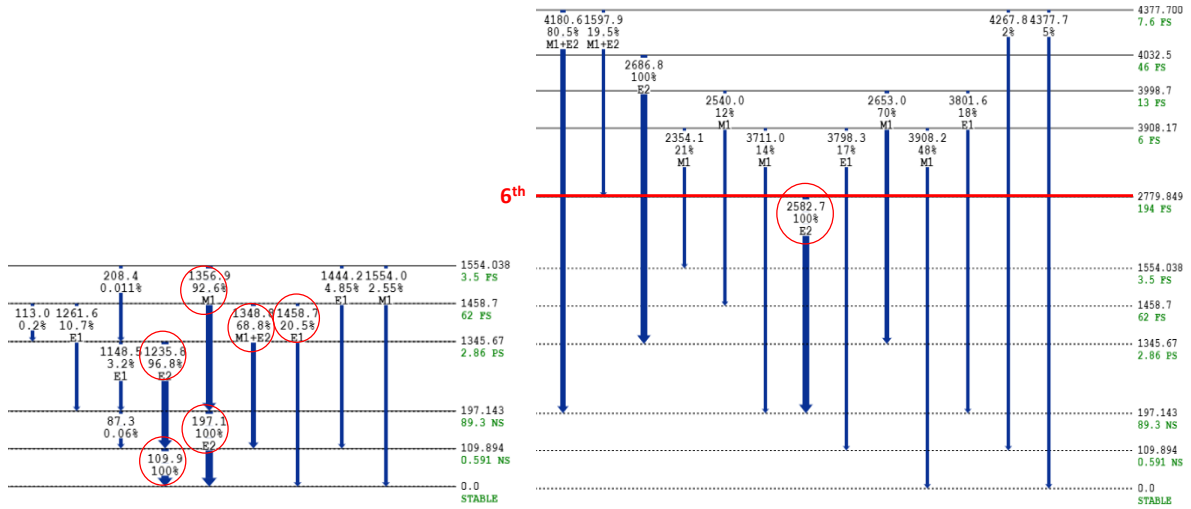


Figure 6: Level scheme of ^{19}F up to the first 10 excited states. According to our simulations, the circled γ -rays are accessible to our measurement and are sufficient to characterise the full cross section up to ~ 4 MeV incident neutron energy.

excited state combined with the fifth excited state, which emits a 1356.9 keV γ -ray. Therefore, in order to make an estimate of the required counting statistics to perform an accurate measurement, the population of these three states alone provides a reasonable approximation.

A Geant4 simulation of a single detector's response to monenergetic γ -ray sources has been performed to calculate a photopeak total efficiency curve. When the efficiency,

branching ratios, predicted partial cross sections and EAR1 flux are taken into account, the expected total detected photopeak γ -rays, summed for the five detectors and for these three key γ -rays are given in Figure 8 for 2×10^{18} protons on target. Also included is an upper estimate for the counts detected from the $(n, 2n)$ reaction; all $(n, 2n)$ reactions have been assumed to result in the emission of a ~ 1 MeV γ -ray however this will not be the case. The ^{18}F may be left in its ground state after the reaction, however currently no calculations have been performed to estimate the probability of this happening. The counting rate estimate has been included primarily for interest here.

Particular focus is put on the 1356.9 keV γ -ray from the fifth excited state, which when combined with the 197.1 keV γ -ray from the second excited is responsible for the majority of the n, n' cross section above 10 MeV. This cannot be resolved from the 1348.8 keV γ -ray however the contribution from this transition is minimal, particularly at higher neutron energies. Using the 1356.9 keV γ -ray as reference, with the suggested 2×10^{18} protons, a minimum of 1000 counts per bin at 25 bins per decade should be detected in the targeted energy region up to 14.1 MeV which would allow the cross section to be determined with an improved accuracy. The binning can be reduced in the high cross section area below 1 MeV, allowing the fine structure present in the cross section to be resolved here.

It is noted that the prominent 197.1 keV γ -ray originates from an isomeric state with a lifetime τ of 89.3 ns, therefore a correction this must be applied which will affect the data, particularly at high neutron energies (low times-of-flight).

In order to measure the seven identified γ -rays with sufficient precision to extract the total (n, n') cross section in the energy range of interest, 2×10^{18} protons are requested.

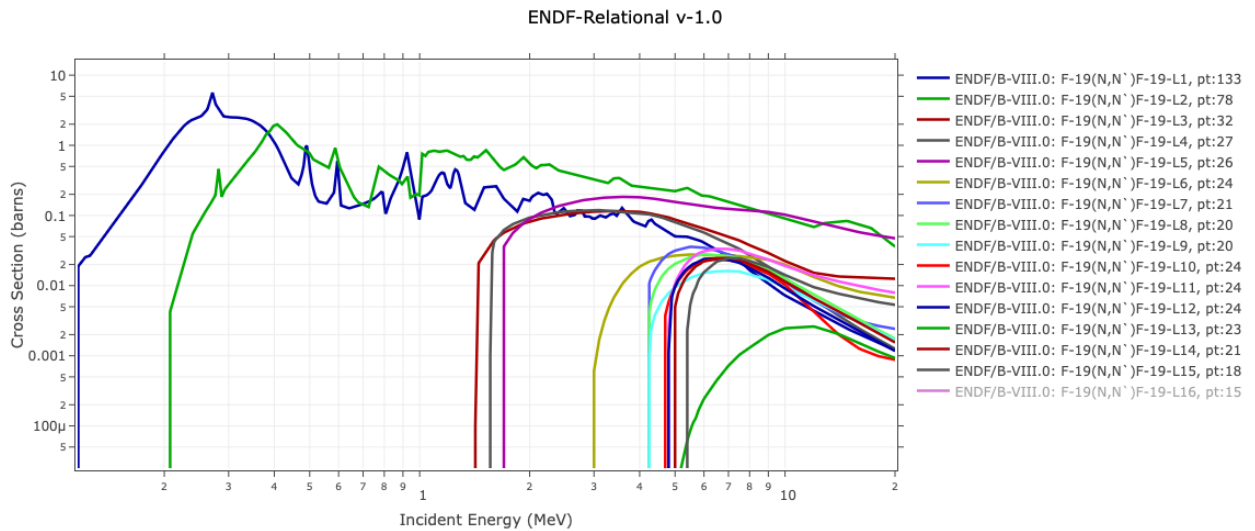


Figure 7: Partial cross section for the population of each excited state in $^{19}\text{F}^*$ as taken from ENDF/B-VIII.0.

Summary of requested protons: 2×10^{18}

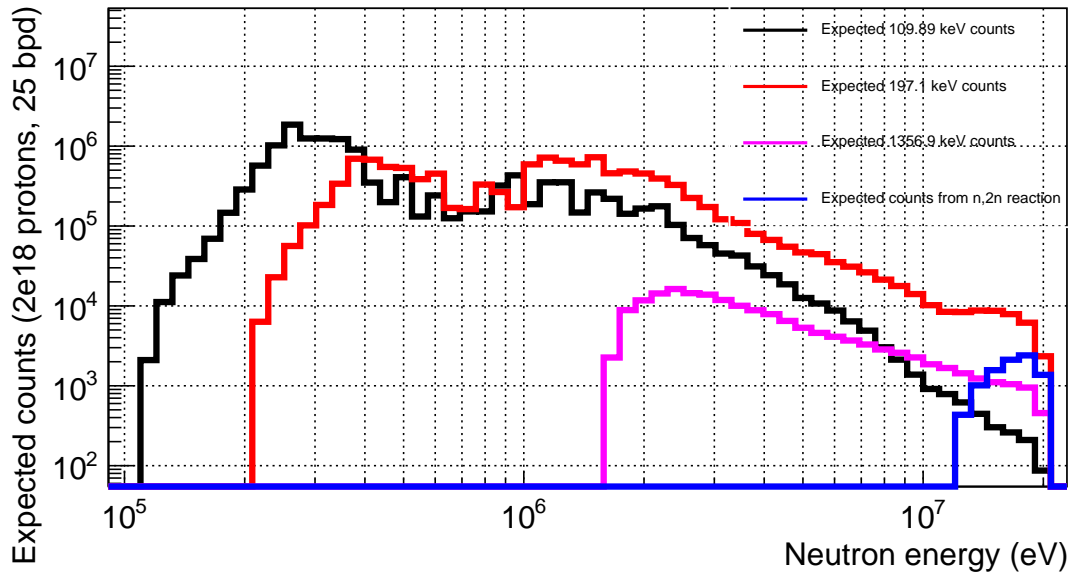


Figure 8: Estimation of the total photopeak detected γ -rays, summed for five detectors, for the three most important transitions of ^{19}F and also the $(n, 2n)$ reaction.

References

- [1] D.L.Broder et al. Cross-sections for γ -quanta production in $(n, n'\gamma)$ reaction on nuclei of fluorine, cobalt, antimony and tantalum. *Fiz.-Energ Institut, Obninsk Reports No.155*, 1969.
- [2] V. C. Rogers. Inelastic neutron scattering in ^{19}F . *Phys. Rev. C*, 9:527–530, Feb 1974.
- [3] Robert B. Day. γ rays from neutron inelastic scattering. *Phys. Rev.*, 102:767–787, May 1956.
- [4] Tim Bohm. Impact of inden f-19 xs in fusion and overview of the fusion evaluated nuclear data library (fendl). *IAEA-National Nuclear Data week 2022, CSEWG validation session*, <https://indico.bnl.gov/event/15497/contributions/70103/attachments/44145/74487/bohmFENDLcsewg2022.pdf>, 2023.
- [5] W.F.G. van Rooijen, Y. Shimazu, and N. Yamano. Criticality uncertainty dependence on nuclear data library in fast molten salt reactors. *Energy Procedia*, 71:3–13, 2015. The Fourth International Symposium on Innovative Nuclear Energy Systems, INES-4.
- [6] Stjärnholm, Sigfrid, Elter, Zsolt, and Sjöstrand, Henrik. Nuclear data uncertainty quantification for reactor physics parameters in fluorine-19-based molten salt reactors. *EPJ Web of Conf.*, 294:05004, 2024.

- [7] Sigfrid Stjärnholm. Propagation of nuclear data uncertainties for reactor physics parameters in fluorine-19-based molten salt reactors. *PhD thesis*, <https://www.diva-portal.org/smash/get/diva2:1780502/FULLTEXT01.pdf>, 2023.
- [8] D.A. Brown et al. ENDF/B-VIII.0: The 8th major release of the nuclear reaction data library with CIELO-project cross sections, new standards and thermal scattering data. *Nuclear Data Sheets*, 148:1 – 142, 2018. Special Issue on Nuclear Reaction Data.

Appendix

DESCRIPTION OF THE PROPOSED EXPERIMENT

Please describe here below the main parts of your experimental set-up:

Part of the experiment	Design and manufacturing
If relevant, write here the name of the <u>fixed</u> installation you will be using [Name fixed/present n_TOF installation: e.g. TAC, C6D6, SIMON, uMegas, HPGe, GEAR-HPGe]	<input checked="" type="checkbox"/> To be used without any modification <input type="checkbox"/> To be modified
If relevant, describe here the name of the <u>flexible/transported</u> equipment you will bring to CERN from your Institute [Part 1 of experiment/ equipment]	<input type="checkbox"/> Standard equipment supplied by a manufacturer <input type="checkbox"/> CERN/collaboration responsible for the design and/or manufacturing
[Part 2 of experiment/ equipment]	<input type="checkbox"/> Standard equipment supplied by a manufacturer <input type="checkbox"/> CERN/collaboration responsible for the design and/or manufacturing
[insert lines if needed]	

HAZARDS GENERATED BY THE EXPERIMENT

Additional hazard from flexible or transported equipment to the CERN site:

Domain	Hazards/Hazardous Activities	Description
Mechanical Safety	Pressure	<input type="checkbox"/> [pressure] [bar], [volume][l]
	Vacuum	<input type="checkbox"/>
	Machine tools	<input type="checkbox"/>
	Mechanical energy (moving parts)	<input type="checkbox"/>
	Hot/Cold surfaces	<input type="checkbox"/>
Cryogenic Safety	Cryogenic fluid	<input type="checkbox"/> [fluid] [m3]
Electrical Safety	Electrical equipment and installations	<input type="checkbox"/> [voltage] [V], [current] [A]
	High Voltage equipment	<input type="checkbox"/> [voltage] [V]
Chemical Safety	CMR (carcinogens, mutagens and toxic to reproduction)	<input type="checkbox"/> [fluid], [quantity]
	Toxic/Irritant	<input type="checkbox"/> [fluid], [quantity]
	Corrosive	<input type="checkbox"/> [fluid], [quantity]
	Oxidizing	<input type="checkbox"/> [fluid], [quantity]
	Flammable/Potentially explosive atmospheres	<input type="checkbox"/> [fluid], [quantity]
	Dangerous for the environment	<input type="checkbox"/> [fluid], [quantity]

Non-ionizing radiation Safety	Laser	<input type="checkbox"/>	[laser], [class]
	UV light	<input type="checkbox"/>	
	Magnetic field	<input type="checkbox"/>	[magnetic field] [T]
Workplace	Excessive noise	<input type="checkbox"/>	
	Working outside normal working hours	<input type="checkbox"/>	
	Working at height (climbing platforms, etc.)	<input type="checkbox"/>	
	Outdoor activities	<input type="checkbox"/>	
Fire Safety	Ignition sources	<input type="checkbox"/>	
	Combustible Materials	<input type="checkbox"/>	
	Hot Work (e.g. welding, grinding)	<input type="checkbox"/>	
Other hazards			